INVESTIGATION OF LINEAR QUADRATIC REGULATOR DECENTRALIZATION PROPERTIES FOR A CLAMPED-CLAMPED BEAM

Zhang, X.[1,2,3], Faria, C.T.[1], Hromcik, M.[2], Hengster-Movric, K.[2]

[1]*Engineering Service, Siemens Industry Software NV*
Interleuvenlaan 68, 3001, Leuven, Belgium
[2]*Dept. Cont. Eng., Fac. Elec. Eng., Czech Tech. Univ. in Prague*
Karlovo namesti 13, 121 35, Prague 2, Czech Republic
[3]*Division PMA, Mech. Eng. Dept., KU Leuven*
Celestijnenlaan 300, BE-3001 Heverlee, Belgium
xueji.zhang@siemens.com

SUMMARY: Heavy computational burden is imposed on centralized controllers when dampening vibration for large-scale flexible structures. For homogeneous flexible structures, the structure of controllers shall be investigated to simplify the control loop design. In this work, firstly a linear-quadratic regulator (LQR) is designed for a normalized infinite-dimensional beam model under a clamped-clamped boundary condition, to demonstrate the decentralization property of the controller. A finite element model (FEM) based on Euler-Bernoulli beam theory is then considered, an LQR is designed with distributed actuators and isolated point-actuators respectively, providing all the states can be measured. Control simulations have shown a decentralization property in both cases, which motivates a decentralized controller inherited from the LQR design. Simulation results have shown that the performance of decentralized controller and the LQR is comparable.

KEYWORDS: PDE FEM LQR decentralized control

1. INTRODUCTION

In centralized control architectures for vibration damping of flexible structures, a considerable computational burden will be imposed on the single centralized controller which is processing measurement information from all the sensors simultaneously. Vibration control for large-scale flexible structures has achieved limited success due to this lack of scalability [6]. For homogeneous structures, the spatially similar dynamics can be taken into account to relax the complexity of controller structures [7]. With the development of advancing technology of micro electro-mechanical systems (MEMS), control with distributed actuator array has regained research interest [8, 9, 10]. In these works, the distributed parameter systems are assumed spatially invariant, hence boundary conditions seem to be a hard problem to tackle, though it is possible to apply the boundary condition on symmetric systems [11, 12]. However, the quadratic controllers designed for these spatially invariant systems exhibit a degree of decentralization or localization [8, 9], which is attractive for a simplified controller design. This feature motivates this work which investigates the decentralization property of optimal linear-quadratic regulator (LQR) for a beam under clamped-clamped boundary condition.
In this work: an LQR is designed for a clamped-clamped homogeneous beam, represented by partial differential equation (PDE) model and finite element model (FEM) respectively. This paper is organized as follows: LQR optimal control design for the PDE model is illustrated in Section 2. LQR design and simulations for the FEM are elaborated in Section 3. Conclusions are drawn in Section 4.

2. PARTIAL DIFFERENTIAL EQUATION (PDE) DEMONSTRATION

In this section the natural decentralization or localization property of an LQR for a normalized PDE model [3] is demonstrated. The clamped-clamped Euler-Bernoulli beam is shown in Figure 1. $w(x,t)$ denotes the deflection of

the beam from its rigid body motion at position x at time t. $u(x,t)$ represents a distributed controlled force along the beam.

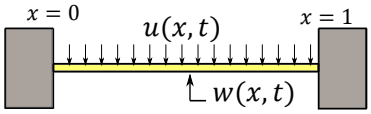

Figure 1 – Clampe-clamped Euler-Bernoulli beam with distributed control input

2.1. PDE model in state-space form

The governing equation for the normalized Euler-Bernoulli beam of unit length with distributed control inputs is given as follows, the beam is clamped at both ends. $w_0(x)$, $\dot{w}_0(x)$ are the initial deflection and velocity profile of the beam respectively.

$$\begin{cases} \frac{\partial^2 w}{\partial t^2}(x,t) = -\frac{\partial^4 w}{\partial x^4}(x,t) + u(x,t), \\ w(x,0) = w_0(x), \\ \frac{\partial w}{\partial t}(x,0) = \dot{w}_0(x), \\ 0 < x < 1, \\ t \geq 0, \end{cases} \tag{1}$$

with boundary conditions

$$\frac{\partial w}{\partial x}(0,t) = \frac{\partial w}{\partial x}(1,t) = w(0,t) = w(1,t) = 0. \tag{2}$$

Define the state variable as $z(\cdot,t) = \begin{bmatrix} w(\cdot,t) \\ \dot{w}(\cdot,t) \end{bmatrix}$. Let

$$\mathbf{L}_\mathbf{2}^\mathbf{s}(0,1) = \begin{array}{l} \{h \in \mathbf{L_2}(0,1) \,|\, h, \frac{dh}{dx}, \frac{d^2h}{dx^2}, \frac{d^3h}{dx^3} \text{ are absolutely continuous,} \\ \frac{d^4h}{dx^4} \in \mathbf{L_2}(0,1), h(0) = \frac{dh(0)}{dx} = 0 = h(1) = \frac{dh(1)}{dx}\}, \end{array} \tag{3}$$

herein, $\mathbf{L_2}(0,1)$ denotes a class of Lebesgue measurable complex-valued functions $\{h(x)\}$with $\int_0^1 |h(x)|^2 dx < \infty$ [3]. Define the state-space $\mathcal{Z} := \mathbf{L}_\mathbf{2}^\mathbf{s}(0,1) \times \mathbf{L_2}(0,1)$. The PDE model can then be reformulated in a state-space form, assuming all the states can be measured:

$$\begin{cases} \dot{z}(\cdot,t) = \mathcal{A}z(\cdot,t) + \mathcal{B}u(\cdot,t), \\ y(\cdot,t) = \mathcal{C}z(\cdot,t), \\ z(\cdot,0) = z_0. \end{cases} \tag{4}$$

Herein $z_0 = \begin{bmatrix} w(\cdot,0) \\ \dot{w}(\cdot,0) \end{bmatrix}$ is the initial states condition and $y(\cdot,t)$ is the measured output, in some Hilbert space: $y \in \mathcal{Y}$. The control effort belongs to an admissible Hilbert space: $u(\cdot,t) \in \mathcal{U}$. The operators are defined as follows:

$$\begin{aligned} \mathcal{A} &:= \begin{bmatrix} \mathbf{0} & I \\ -\frac{d^4}{dx^4} & \mathbf{0} \end{bmatrix} \in \mathcal{L}(\mathcal{Z}, \mathbf{L_2}(0,1) \times \mathbf{L}_\mathbf{2}^\mathbf{s}(0,1)) \\ \mathcal{B} &:= \begin{bmatrix} \mathbf{0} \\ I \end{bmatrix} \in \mathcal{L}(\mathcal{U}, \mathbf{L_2}(0,1) \times \mathbf{L}_\mathbf{2}^\mathbf{s}(0,1)) \\ \mathcal{C} &:= I \in \mathcal{L}(\mathcal{Z}, \mathcal{Y}). \end{aligned} \tag{5}$$

Herein I is the *identity* operator defined on respective Hilbert spaces, $\mathcal{L}(\mathbf{X}, \mathbf{Y})$ denotes a set of bounded linear operators mapping from $\mathbf{X}$ to $\mathbf{Y}$.

2.2. Eigenfunctions (Eigenmodes)

Eigenfunctions or vibration eigenmodes form an important basis of the state-space. They can be used to solve the algebraic riccati equation (ARE) associated with the LQR problem, which will be illustrated in Section 2.3. Defining the linear operator $\mathcal{A}_0 := \frac{d^4}{dx^4} \in \mathcal{L}(\mathbf{L}_\mathbf{2}^\mathbf{s}(0,1))$, where $\mathcal{L}(\mathbf{X})$ denotes a set of bounded linear operators from $\mathbf{X}$

to $\mathbf{X}$. The eigen-function and eigen-value of $\mathcal{A}_0$ are denoted by h and γ respectively. By solving the eigen-problem

$$\mathcal{A}_0 h = \frac{d^4}{dx^4} h = \gamma h, \tag{6}$$

the following equations hold:

$$\begin{gathered} \gamma_n = k_n^4 \\ h_n(x) = p_n\{\cos(k_n x) - \cosh(k_n x) - \tfrac{\cos(k_n)-\cosh(k_n)}{\sin(k_n)-\sinh(k_n)}[\sin(k_n x) - \sinh(k_n x)]\}, \end{gathered} \tag{7}$$

where p_n is an arbitrary real scalar, and k_n satisfies the equation

$$1 - \cos(k_n)\cosh(k_n) = 0. \tag{8}$$

Through simple calculation, the eigen-value λ and eigen-function φ of the operator $\mathcal{A}$, associated with the eigen-problem

$$\mathcal{A}\varphi = \lambda\varphi, \tag{9}$$

can be derived as:

$$\lambda_n = j\sqrt{\gamma_n}, \tag{10}$$

and

$$\varphi_n(x) = \begin{bmatrix} \frac{1}{\lambda_n} h_n(x) \\ h_n(x) \end{bmatrix} := \begin{bmatrix} \eta_n(x) \\ h_n(x) \end{bmatrix}. \tag{11}$$

2.3. LQR formulation

The LQR control problem is formulated as

$$\begin{aligned} &\underset{u(\cdot,t)}{\text{minimize}}\, J(z_0; u(\cdot,t)) := \int_0^\infty (< y, y >_{\mathcal{Y}} + < u, \mathcal{R}u >_{\mathcal{U}}) dt \\ &\text{subject to} \begin{cases} \dot{z}(\cdot,t) = \mathcal{A}z(\cdot,t) + \mathcal{B}u(\cdot,t) \\ y(\cdot,t) = \mathcal{C}z(\cdot,t). \end{cases} \end{aligned} \tag{12}$$

Herein $< \cdot, \cdot >_{\mathcal{H}}$ is an *inner product* on an associated Hilbert space $\mathcal{H}$. In the following text, without causing ambiguity, the subscript of the *inner product* is omitted for simplicity. $\mathcal{R}$ is a weighting *self-adjoint* operator acting on $u(\cdot,t)$ [3]. The optimal control is given as

$$u_{min} = -\mathcal{R}^{-1}\mathcal{B}^*\Pi z_{min}, \tag{13}$$

where z_{min} is the corresponding optimal state trajectory under optimal control u_{min}, $\mathcal{B}^*$ is the *adjoint operator* of $\mathcal{B}$, Π is a *self-adjoint operator* acting on $\mathcal{Z}$ that satisfies the following ARE [3]:

$$< \mathcal{A}z_1, \Pi z_2 > + < \Pi z_1, \mathcal{A}z_2 > + < \mathcal{C}z_1, \mathcal{C}z_2 > - < \Pi z_1, \mathcal{B}\mathcal{R}^{-1}\mathcal{B}^*\Pi z_2 >= 0, \forall z_1, z_2 \in \mathcal{Z}. \tag{14}$$

Seek Π of the form:

$$\Pi z := \Sigma_{n,m=1}^{\infty} \Pi_{nm} < z, \varphi_m > \varphi_n, \tag{15}$$

herein φ_n, φ_m are the orthonormal eigenfunctions of the operator $\mathcal{A}$ (See the details in Appendix A). Thereby

$$\Pi_{nm} =< \varphi_n, \Pi\varphi_m > . \tag{16}$$

Take $z_1 = \varphi_n$, $z_2 = \varphi_m$, substitute into the ARE (Equation (14), here $\mathcal{R} = I$, the control efforts are equally weighted along the beam), then

$$(\lambda_n + \overline{\lambda_m})\Pi_{nm} + \delta_{nm} - < \Pi\varphi_n, \begin{bmatrix} \mathbf{0} & \mathbf{0} \\ \mathbf{0} & I \end{bmatrix} \Pi\varphi_m >= 0, \tag{17}$$

where δ_{nm} is the Kronecker delta function: $\delta_{nm} = \begin{cases} 1, \text{ if } n = m \\ 0, \text{ if } n \neq m \end{cases}$. Let

$$\Pi = \begin{bmatrix} \Pi_1 & \Pi_2 \\ \Pi_3 & \Pi_4 \end{bmatrix}, \tag{18}$$

where $\Pi_1 \in \mathcal{L}(\mathbf{L_2^s}(\mathbf{0},\mathbf{1}))$, $\Pi_2 \in \mathcal{L}(\mathbf{L_2}(\mathbf{0},\mathbf{1}),\mathbf{L_2^s}(\mathbf{0},\mathbf{1}))$, $\Pi_3 \in \mathcal{L}(\mathbf{L_2^s}(\mathbf{0},\mathbf{1}),\mathbf{L_2}(\mathbf{0},\mathbf{1}))$, and $\Pi_4 \in \mathcal{L}(\mathbf{L_2}(\mathbf{0},\mathbf{1}))$. Combining Equation (11), the Equation (17) becomes:

$$(\lambda_n + \overline{\lambda_m})\Pi_{nm} + \delta_{nm} - < \Pi_3\eta_n + \Pi_4 h_n, \Pi_3\eta_m + \Pi_4 h_m >= 0. \tag{19}$$

Combining Equation (11), (16) and (18):

$$\Pi_{nm} = \frac{1}{\lambda_n\overline{\lambda_m}} < h_n, \Pi_1 h_m > + \frac{1}{\lambda_n} < h_n, \Pi_2 h_m > + \frac{1}{\overline{\lambda_m}} < h_n, \Pi_3 h_m > + < h_n, \Pi_4 h_m > . \tag{20}$$

Moreover, since Π is a *self-adjoint* operator *i.e.* $\Pi = \Pi^*$, there is (Proof is omitted due to triviality):

$$\begin{array}{l} \Pi_1^* = \Pi_1, \\ \Pi_2^* = \Pi_3, \\ \Pi_3^* = \Pi_2, \\ \Pi_4^* = \Pi_4. \end{array} \tag{21}$$

By inspecting Equation (19), (20) and (21), seek Π such that $\Pi_1 = I$, $\Pi_2 = 0$, $\Pi_3 = 0$ and Π_4 is a $Riesz-spectral$ operator [3] with eigenvalues $\{\beta_n\}$ and eigenfunctions $\{h_n\}$:

$$\Pi_4 := \Sigma_{n=1}^{\infty}\beta_n < \cdot, \zeta_n > h_n, \tag{22}$$

where ζ_n is the scaled eigenfunction of Π_4^* (hence Π_4) such that $< \zeta_n, h_m >= \delta_{nm}$, in fact,

$$\zeta_n = \frac{1}{\|h_n\|^2} h_n. \tag{23}$$

Hence Equation (19) turns into:

$$(\lambda_n + \overline{\lambda_m})(\overline{\beta_m} + \frac{1}{\lambda_n\overline{\lambda_m}}) < h_n, h_m > + \delta_{nm} - \beta_n\overline{\beta_m} < h_n, h_m >= 0. \tag{24}$$

When $n \neq m$, due to orthogonality of h_n (See Appendix A.1), the above equation holds. When $n = m$, note $\lambda_n = j\sqrt{\gamma_n}$, Equation (24) becomes:

$$1 - \|\beta_n\|^2\|h_n\|^2 = 0, \tag{25}$$

thereby,

$$\beta_n = \frac{1}{\|h_n\|} = \frac{\sqrt{1+k_n^4}}{k_n^2}. \tag{26}$$

2.4. Convolution Kernel

Following Equation (13), the optimal control input is given as

$$u_{min} = -\Pi_4\dot{w} = -\Sigma_{n=1}^{\infty}\beta_n < \dot{w}, \zeta_n > h_n = -\Sigma_{n=1}^{\infty}\alpha_n < \dot{w}, h_n > h_n, \tag{27}$$

where $\alpha_n = \frac{1}{\|h_n\|^3}$, and the last equation holds due to Equation (23). The feedback convolution kernel $\mathcal{K}(x,\xi)$ is defined implicitly as follows:

$$u = -\int_0^1 \mathcal{K}(x,\xi)\dot{w}(\xi)d\xi. \tag{28}$$

The convolution kernel for the optimal control can be calculated by the following equation:

$$\begin{array}{l} u_{min} = -\Sigma_{n=1}^{\infty}\alpha_n < \dot{w}, h_n > h_n = -\Sigma_{n=1}^{\infty}\alpha_n \int_0^1 h_n(x)h_n(\xi)\dot{w}(\xi)d\xi \\ \quad = -\int_0^1 \Sigma_{n=1}^{\infty}\alpha_n h_n(x)h_n(\xi)\dot{w}(\xi)d\xi = -\int_0^1 \mathcal{K}(x,\xi)\dot{w}(\xi)d\xi. \end{array} \tag{29}$$

Hence,

$$\mathcal{K}(x,\xi) = \Sigma_{n=1}^{\infty}\alpha_n h_n(x)h_n(\xi). \tag{30}$$

2.5. Numerical evaluation

For evaluation, eigenfunctions $\{h_n\}$ are found numerically by solving Equation (8). The convolution kernel is approximated via truncated expansions of the eigenfunctions: $\overline{\mathcal{K}}(x,\xi) = \Sigma_{n=1}^{N_{tr}} \alpha_n h_n(x) h_n(\xi)$. The kernel profiles for different N_{tr} and locations are shown in Figure 2. It can be seen that as N_{tr} increases, the degree of localization also increases. This fact shows the decentralization of the distributed controllers: the localized control action mainly depends on neighbouring measurement information from the distributed sensors; also, the more eigenfunctions (or vibration modes) are considered in the modeling phase, the more decentralized the LQR designed in the control phase will be.

This property can be roughly reasoned as follows: numerically k_n grows quickly as n increases, hence $\|h_n\|^2 = \frac{k_n^4}{1+k_n^4} \approx 1$, hence h_n are almost orthonormal eigenfunctions. From Equation (27), it can be deduced that Π_4 is almost an *identity* operator. By comparing Equation (28), it can be seen that:

$$\mathcal{K}(x,\xi) \approx \delta(x-\xi). \tag{31}$$

The convolution kernel is almost a Dirac delta function, which is in accordance with the decentralization property.

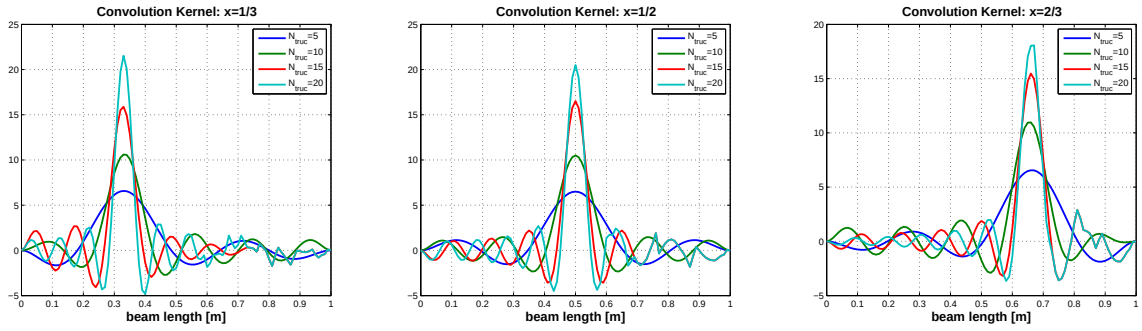

(a) $x = 1/3$ (b) $x = 1/2$ (c) $x = 2/3$

Figure 2 – Profiles of the convolution kernel at different locations

3. FEM DEMONSTRATION

A finite element model of a clamped-clamped beam is considered in this section. For simplicity, the dynamics of actuators and sensors have been omitted.

3.1. Mechanical structure modeling

The finite element model of the beam with clamped-clamped boundary condition has been constructed based on the Euler-Bernoulli beam theory. Each beam element has two nodes. At each node, two degrees of freedom have been considered, i.e. deflection w and slope $\frac{\partial w}{\partial x}$ [1, 2]. The physical parameters used in the finite element model of the beam are shown in Table 1. The number of elements in the model is 50. After assembling all the element matrices, the dynamic equation of the global beam can be written as:

Parameter	Value
Length	$1\ m$
Width	$0.1\ m$
Thickness	$0.001\ m$
Density	$10\ kg/m^3$
Young's Modulus	$0.1\ GPa$
Modal damping ratio	5×10^{-5}

Table 1 – Parameter table

$$\mathbf{M\ddot{q}(t)} + \mathbf{Kq(t)} = \mathbf{L_u u(t)}, \tag{32}$$

where $\mathbf{q(t)}$ denotes the displacement, $\mathbf{M}$ and $\mathbf{K}$ represent global mass matrix and global stiffness matrix respectively, and $\mathbf{L_u}$ is the localization matrix for external control inputs.

3.2. Modal model in state-space form

The solution of the dynamic equation is given $\mathbf{q(t)} = \phi e^{j\omega t}$. ϕ and ω must satisfy the eigen-problem

$$(\mathbf{K} - \omega^2 \mathbf{M})\phi = 0. \tag{33}$$

The solution generates the natural frequencies denoted by ω_i and the corresponding mode shapes denoted by ϕ_i. The matrix of the mode shapes is defined as

$$\Phi = \begin{pmatrix} \phi_1 & \phi_2 & \cdots & \phi_n \end{pmatrix}, \tag{34}$$

n is the dimension of matrices $\mathbf{M}$ and $\mathbf{K}$. With the linear transform $\mathbf{q} = \Phi \mathbf{q_m}$, the dynamic equation is then transformed to

$$\mathbf{M_m \ddot{q}_m(t)} + \mathbf{K_m q_m(t)} = \Phi^T \mathbf{L_u u}((\mathbf{t}). \tag{35}$$

Herein $\mathbf{M_m} = \Phi^T M \Phi$, $\mathbf{K_m} = \Phi^T K \Phi$ are diagonal matrices. To make the dynamic equations more realistic, a damping term is added. In modal coordinates, the damping matrix can be conveniently evaluated and the damping estimation is usually more accurate than in nodal coordinates [4]. Hence the dynamic equation in modal coordinates turns into:

$$\mathbf{M_m \ddot{q}_m(t)} + \mathbf{C_m \dot{q}_m(t)} + \mathbf{K_m q_m(t)} = \Phi^T \mathbf{L_u u}((\mathbf{t}). \tag{36}$$

For numerical simulations in later sections, the damping ratios for all the modes are taken equally as $\zeta_i = 5 \times 10^{-5}$. For control system analysis and design purposes, the modal model is normally represented in a state-state form. Defining the state variable consisting of modal displacement and velocities:

$$x = \begin{pmatrix} x_1 \\ x_2 \end{pmatrix} = \begin{pmatrix} \mathbf{q_m} \\ \mathbf{\dot{q}_m} \end{pmatrix}, \tag{37}$$

the modal model in the state-space form is:

$$\begin{cases} \dot{x}(t) = Ax(t) + Bu(t), \\ y(t) = Cx(t). \end{cases} \tag{38}$$

Herein $y(t)$ is the controlled output, A and B are as follows:

$$A = \begin{pmatrix} \mathbf{0} & I \\ -\mathbf{M_m^{-1}K} & -\mathbf{M_m^{-1}C_m} \end{pmatrix}, \quad B = \begin{pmatrix} \mathbf{0} \\ \Phi^T \mathbf{L_u} \end{pmatrix}. \tag{39}$$

3.3. LQR control formulation

The infinite-horizon continuous-time LQR problem is formulated as to find the control input $u(t)$ such that minimises the cost index:

$$J := \int_0^\infty [y(t)^T y(t) + u(t)^T R u(t)] dt = \int_0^\infty [x(t)^T Q x(t) + u(t)^T R u(t)] dt, \tag{40}$$

where $Q = C^T C \succeq 0$, $R \succeq 0$ are the penalty symmetric matrices for states and control efforts respectively. The state feedback control law $u = -Fx$ that minimises J is given by

$$F = R^{-1} B^T P, \tag{41}$$

and $P \succ 0$ is the solution of the Algebraic Riccati Equation (ARE):

$$A^T P + PA - PBR^{-1} B^T P + Q = 0. \tag{42}$$

3.4. Control simulations

Three different simulation cases are demonstrated through Section 3.4.1-3.4.3. The LQR optimal control simulation are carried out in two scenarios. The first one is assuming that at each node of the finite-element model, there are two control variables in the form of force (f) and torque (τ), corresponding to w and $\frac{\partial w}{\partial x}$ respectively. Another case is considered that there are only force inputs and can be applied only at finite nodes. In addition, a decentralization configuration is then constructed to investigate the close-loop performance. For all control simulations, the same initial condition is applied: contribution of first 15 modes with equal modal coordinates 1×10^{-5} to the initial profile of the beam.

3.4.1. *Distributed Actuators and Sensors*

In this distributed case, it is assumed ideally that both measurements ($\mathbf{q}$ and $\dot{\mathbf{q}}$) and control inputs (f and τ) are distributed at each nodes. For the numerical simulation, Q and R are tuned as follows:

$$Q = \begin{pmatrix} I & \mathbf{0} \\ \mathbf{0} & 0.01I \end{pmatrix}, R = 0.01I. \tag{43}$$

The closed-loop displacement of all the nodes is shown in Figure 3a, and the open-loop beam vibration is as shown in Figure 3b. Not surprisingly, with full state feedback, the system can be regulated very well. Since the degree of "decentralization" is of more interest, the structure of the static feedback gain matrix is then investigated:

$$u = -Fx = \begin{pmatrix} F_{m1} & F_{m2} \end{pmatrix} \begin{pmatrix} \mathbf{q_m} \\ \dot{\mathbf{q}}_\mathbf{m} \end{pmatrix} = \begin{pmatrix} F_{m1}\Phi^{-1} & F_{m2}\Phi^{-1} \end{pmatrix} \begin{pmatrix} \mathbf{q} \\ \dot{\mathbf{q}} \end{pmatrix} = \begin{pmatrix} F_1 & F_2 \end{pmatrix} \begin{pmatrix} \mathbf{q} \\ \dot{\mathbf{q}} \end{pmatrix}. \tag{44}$$

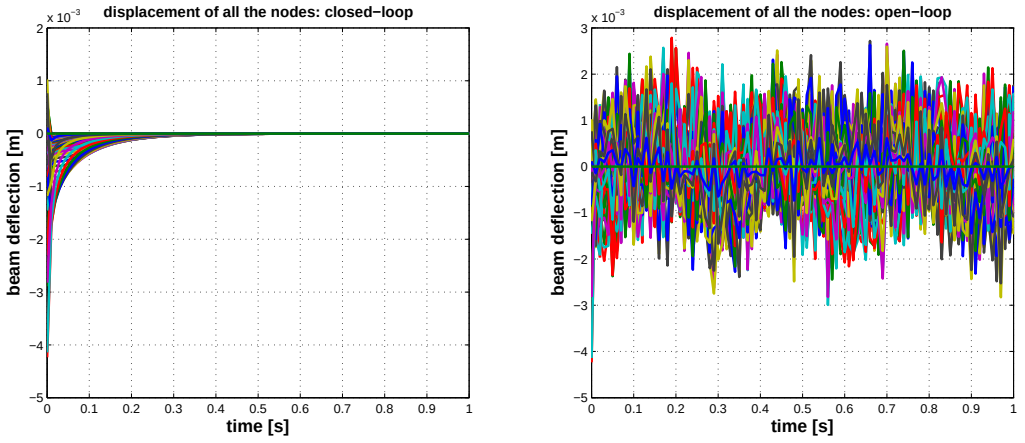

(a) Closed-loop nodes position

(b) Open-loop nodes position

Figure 3 – LQR closed-loop and open-loop beam vibration

For the ease of demonstration, f_{1z}, f_{2z}, $f_{1\theta}$, $f_{2\theta}$ represent the feedback matrices generating force from w, $\frac{dw}{dt}$, $\frac{\partial w}{\partial x}$ and $\frac{d(\frac{\partial w}{\partial x})}{dt}$ respectively, and τ_{1z}, τ_{2z}, $\tau_{1\theta}$, $\tau_{2\theta}$ represent the feedback matrices generating torque from w, $\frac{dw}{dt}$, $\frac{\partial w}{\partial x}$ and $\frac{d(\frac{\partial w}{\partial x})}{dt}$ respectively. All of these eight matrices can be extracted from F_1 and F_2. The spatial distributions of f_{1z} and $\tau_{2\theta}$ are shown in Figure 4a and Figure 4b. It can be seen that both matrices are diagonally dominant. The other matrices which have been omitted due to space have shown in a similar way. This feature shows the inherited decentralization property of the LQR.

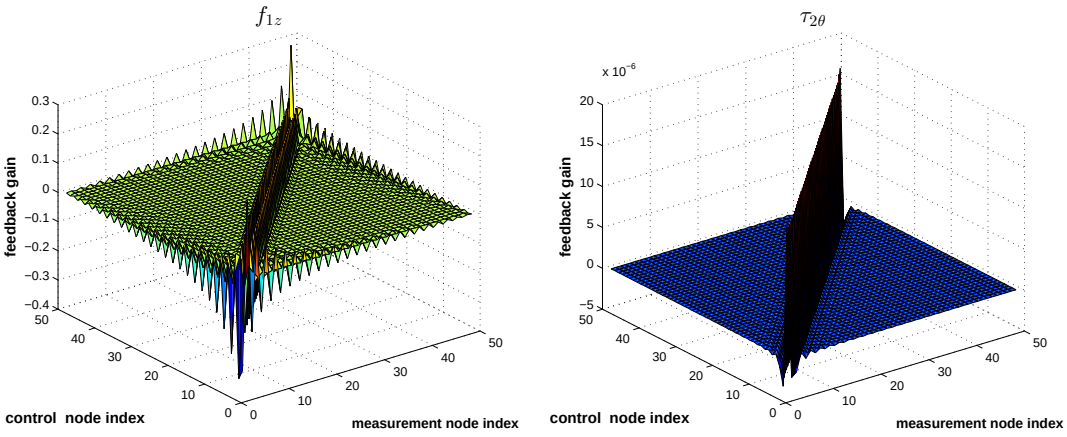

(a) f_{1z} distribution

(b) $\tau_{2\theta}$ distribution

Figure 4 – Feedback spatial distribution

3.4.2. *Discrete Actuators and Distributed Sensors*

In this section, the rigorous assumption of distributed control inputs is relxed to force inputs only and applied at a finite number of nodes. For the following numerical simulation, the control input locations on the beam are assumed at $x = \frac{1}{3}, \frac{1}{2}, \frac{2}{3}$. For the numerical simulation, Q and R are tuned as follows:

$$Q = \begin{pmatrix} I & \mathbf{0} \\ \mathbf{0} & 0.1I \end{pmatrix}, R = 0.1I. \tag{45}$$

The closed-loop simulation is shown in Figure 5. It can be seen that though very limited control variables and control locations are allowed, with full state feedback, the closed-loop system can still perform very well.

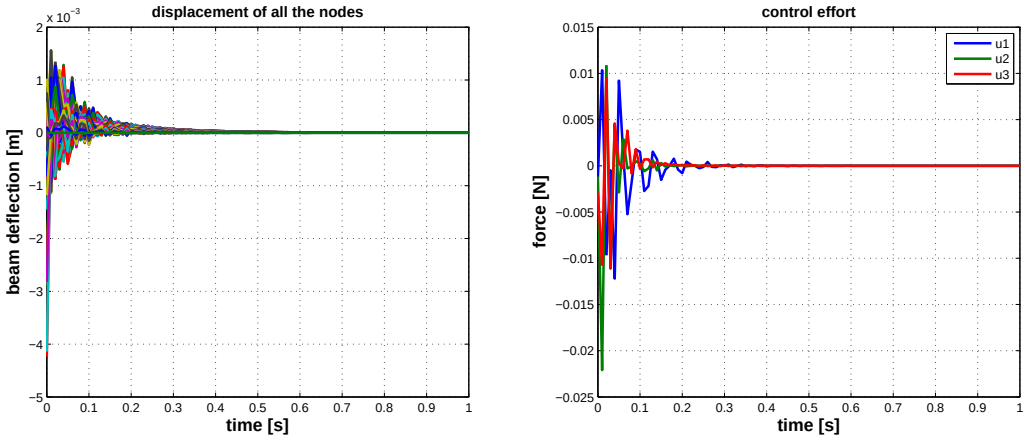

(a) Closed-loop nodes position

(b) Closed-loop control effort

Figure 5 – Closed-loop simulation: discrete actuators, distributed sensors

Similar to the previous simulation scenario, f_{1z} and f_{2z} are shown in Figure 6a and Figure 6b. It seems that the diagonally dominance property still holds in this simulation. Hence it is reasonable to investigate the performance with the decentralized configuration, which will be shown in the next section.

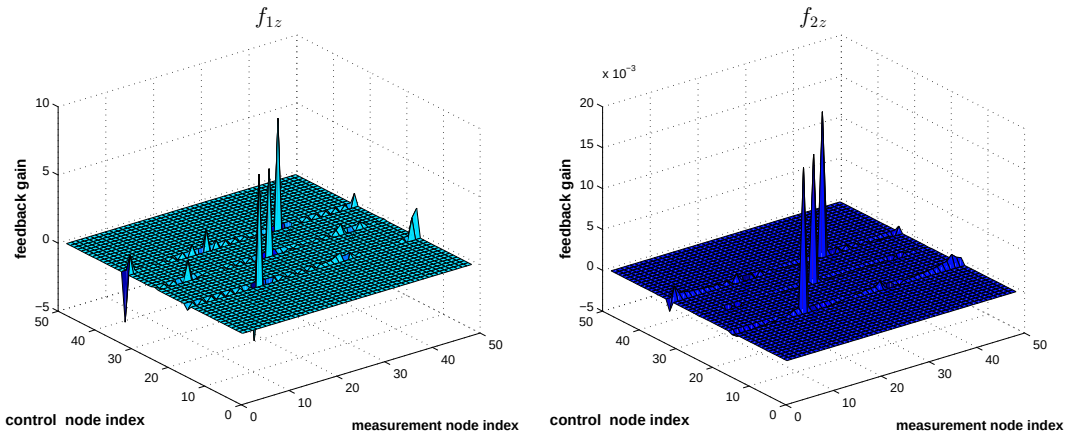

(a) f_{1z} distribution

(b) f_{2z} distribution

Figure 6 – Feedback gain spatial distribution for discrete actuators and distributed sensors

3.4.3. *Discrete Actuators and Sensors*

In this simulation scenario, the control input configuration remains the same as in the previous simulation. However, it is assumed that only velocity localized at the control points can be measured. Furthermore, each local measurement is accessible only to the local control input, namely the closed-loop is in a simple *collocated control* configuration [5]. The local feedback gain is inherited from the previous simulation scenario. The stability of the closed-loop is guaranteed since the velocity feedback is equivalent to adding damping term to the dynamic system [5]. The closed-loop performance is shown in Figure 7. Compared with previous simulation scenarios, the system is stabilized in a comparable time, though the collocated controller is much more simplified. This gives a hint for the future implementation: once the collocated control points are fixed, the local feedback gain attained via full state feedback LQR design can serve as a starting estimation for the practical parameter tuning, providing that the structural dynamic modeling is accurate enough.

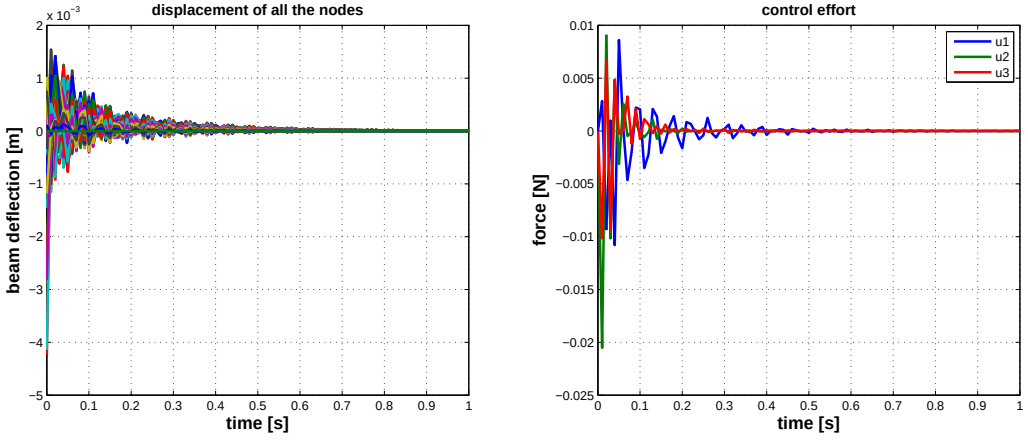

(a) Closed-loop nodes position

(b) Closed-loop control effort

Figure 7 – Closed-loop simulation, collocated configuration

4. CONCLUSIONS

In this work, LQR control design for a clamped-clamped homogeneous Euler-Bernoulli beam is investigated. For the PDE model, through analytical derivation and numerical evaluation, it shows that the convolution kernel is

almost a Dirac delta function, so LQR has an inherited decentralization property. For the finite element model, LQR design for different actuator configurations is carried out, both controllers show a degree of localization throughout the space. The decentralized control with feedback parameters inherited from the LQR design is then studied, and simulation shows that the closed-loop performance has no obvious degradation. This sheds light on the possibility of reducing the computation load of the central computer while preserving the damping performance.

A. ORTHONORMALIZATION OF EIGENFUNCTIONS

A.1. Orthogonality of h_n

Since $\mathcal{A}_0 := \frac{d^4}{dx^4} \in \mathcal{L}(\mathbf{L}_2^{\mathbf{s}}(0,1))$, for any vectors $a, b \in \mathbf{L}_2^{\mathbf{s}}(0,1)$, the *inner product* $< a,b >$ is defined as $< a,b >:= \int_0^1 a(x)\overline{b}(x)dx$. With integration by parts:

$$< \mathcal{A}_0 a, b >= \int_0^1 \frac{d^4a(x)}{dx^4}\overline{b}(x)dx = \frac{d^3a(x)}{dx^3}\overline{b}(x)\Big|_0^1 - \frac{d^2a(x)}{dx^2}\frac{d\overline{b}(x)}{dx}\Big|_0^1 + \frac{d^2\overline{b}(x)}{dx^2}\frac{da(x)}{dx}\Big|_0^1 - \frac{d^3\overline{b}}{dx^3}a(x)\Big|_0^1 + \int_0^1 a(x)\frac{d^4\overline{b}(x)}{dx^4}dx \tag{46}$$

Due to the boundary conditions:

$$< \mathcal{A}_0 a, b >= \int_0^1 a(x)\frac{d^4\overline{b}(x)}{dx^4}dx =< a, \mathcal{A}_0 b > \tag{47}$$

Hence $\mathcal{A}_0$ is a *self-adjoint* operator. Easy to see:

$$\gamma_m < h_m, h_n >=< \mathcal{A}_0 h_m, h_n >=< h_m, \mathcal{A}_0 h_n >= \gamma_n < h_m, h_n > .$$

Thereby

$$(\gamma_m - \gamma_n) < h_m, h_n >= 0. \tag{48}$$

For $n \neq m$, there is $\gamma_m \neq \gamma_n$, from Equation (48), it can be derived that $< h_m, h_n >= 0, \forall m \neq n$.

A.2. Orthonormalization of φ_n

For the Hilbert space $\mathcal{Z} = \mathbf{L}_2^{\mathbf{s}}(0,1) \times \mathbf{L}_2(0,1)$, for any vectors c_1, $d_1 \in \mathbf{L}_2^{\mathbf{s}}(0,1)$, c_2, $d_2 \in \mathbf{L}_2(0,1)$, and $c = \begin{bmatrix} c_1 \\ c_2 \end{bmatrix}$, $d = \begin{bmatrix} d_1 \\ d_2 \end{bmatrix}$, the *inner product* is defined as:

$$< c, d >_{\mathcal{Z}} := \int_0^1 c_1(x)\overline{d_1}(x)dx + \int_0^1 c_2(x)\overline{d_2}(x)dx. \tag{49}$$

Hence for any two eigenfunctions of the operator $\mathcal{A}$, the inner product is

$$< \varphi_n, \varphi_m >_{\mathcal{Z}} = (\frac{1}{\lambda_n\overline{\lambda_m}} + 1) < h_n, h_m > . \tag{50}$$

For $n \neq m$, $< \varphi_n, \varphi_m >_{\mathcal{Z}} = 0$. When $n = m$,

$$< \varphi_n, \varphi_n >_{\mathcal{Z}} = (1 + \frac{1}{\gamma_n})\|h_n\|^2 = (1 + \frac{1}{k_n^4})\|h_n\|^2 \tag{51}$$

By scaling h_n (changing parameter p_n in Equation (7)) such that $\|h_n\|^2 = \frac{k_n^4}{1+k_n^4}$, orthonormal eigenfunctions can be obtained:

$$< \varphi_n, \varphi_m >_{\mathcal{Z}} = \delta_{nm} = \begin{cases} 1, \text{ if } n = m \\ 0, \text{ if } n \neq m \end{cases} \tag{52}$$

ACKNOWLEDGEMENTS

The authors greatly appreciate the support of the European Commission under the Marie Curie Fellowship: FP7-PEOPLE-2013-ITN-EID-ARRAYCON.

REFERENCES

[1] Petyt, M., "Introduction to Finite Element Vibration Analysis", Second edition, Cambridge University Press,2010.

[2] Ferreira, A.J.M., "MATLAB Codes for Finite Element Analysis, Solids and Structures", Springer, 2008.

[3] Curtain, R.F., Zwart, H.J., "An Introduction to Infinite-Dimensional Linear Systems Theory", Springer-Verlag, 1995.

[4] Gawronski, W.K., "Advanced Structural Dynamics and Active Control of Structures", Springer-Verlag, 2004.

[5] Preumont, A., "Vibration Control of Active Structures: An Introduction", Second edition, KLUWER ACADEMIC PUBLISHERS, 2002.

[6] Frampton, K.D., Baumann, O.N., Gardonio, P., "A comparison of decentralized, distributed, and centralized vibro-acoustic control", J. Acoust. Soc. Am, 128, 2010, pp. 2798-2806.

[7] Ayres, G., Paganini, F., "Convex Method for Localized Control Design in Spatially Invariant Systems", Proc. IEEE Conference on Decision and Control, 2000, pp. 3751-3756.

[8] Bamieh, B., Paganini, F., Dahleh, M. A., "Distributed Control of Spatially Invariant Systems", IEEE Trans. on Autom. Control, 15(1), 2001, pp. 129-137.

[9] Paganini, F., Bamieh, B., "Decentralization Properties of Optimal Distributed Controllers", Proc. IEEE Conference on Decision and Control, 1998, pp. 1877-1882.

[10] D'Andrea, R., Dullerud, G.E., "Distributed Control Design for Spatially Interconnected Systems", IEEE Trans. on Autom. Control, 48, 2003, pp. 1478-1495.

[11] Langbort, C., D'Andrea, R., "Distributed Control of Spatially Reversible Interconnected Systems with Boundary Conditions", SIAM J. on Control and Optimization, 44, 2004, pp. 1-28.

[12] Scholte, E., D'Andrea, R., "Active Vibro-acoustic Control of a Flexible Beam Using Distributed Control", Proc. of the America Control Conference, 2003, pp. 2640-2645.